Relaxation to Maxwellian equilibrium in a periodic kinetic model

Payam Danesh [1]†, Raoul Bianchetti [2]†

[1] Department of biosystems Engineering, University of Tehran, Iran. Payamdanesh71@gmail.com

[2] Information Physics Institute, Gosport, Hampshire, United Kingdom. raoul.bianchetti@informationphysicsinstitute.net

† These authors contributed equally to this work

Abstract

We study a periodic kinetic Fokker–Planck equation in which free transport in position is coupled to Ornstein–Uhlenbeck relaxation in velocity. Our aim is to give a transparent weighted L^2 analysis of the relaxation mechanism and to test it by a modal approximation. The equation is written in Maxwellian variables, the generator is decomposed into a skew transport part and a dissipative velocity part and its contraction semigroup is considered on the natural weighted Hilbert space. Using Gaussian and torus Poincaré inequalities, we prove mass conservation, microscopic coercivity and exponential decay on the zero-mass subspace through a modified first-order energy containing a spatial–velocity cross term. For the homogeneous problem, the entropy identity gives decay from the Gaussian logarithmic Sobolev inequality. A Fourier–Hermite discretization is then derived, its semi-discrete L^2-stability is shown and truncation tests quantify convergence in the Hermite index and the spectral abscissa of the first nonzero Fourier block. The results give a compact account of how velocity relaxation enforces global return to Maxwellian equilibrium in this model.

Keywords: Kinetic Fokker–Planck equation; Maxwellian equilibrium; hypocoercive relaxation

1. Introduction

Kinetic Fokker–Planck equations describe probability densities on phase space [1] as they combine deterministic motion in position with diffusion and friction in velocity. The mathematical roots of this class of problems go back to Kolmogoroff's early work on Brownian motion and degenerate diffusion [2] and to Kramers' phase-space description of Brownian particles in a force field [3]. Hörmander's hypoellipticity theorem later clarified how commutators can compensate for missing diffusion directions [4]. Also Gross' logarithmic Sobolev inequality became a fundamental tool for entropy dissipation under Gaussian measures [5], while Risken's monograph remains a standard reference for the derivation, solution methods, and applications of Fokker–Planck equations in physics and chemistry [6]. In the last two decades, the modern quantitative theory of convergence to equilibrium for degenerate kinetic equations developed rapidly. For example, Hérau and Nier proved hypoellipticity and trend to equilibrium for Fokker–Planck equations with confining potentials [7]. Mouhot and Neumann established perturbative convergence estimates for collisional kinetic equations on the torus [8]. Villani's memoir gave a systematic hypocoercivity framework based on adapted Lyapunov functionals and commutator structures [9]. later Dolbeault, Mouhot, and Schmeiser formulated an efficient abstract method for linear kinetic equations conserving mass [10].

Having previous works, the contribution of this paper is the precise assembly of the full argument for the concrete periodic transport–Ornstein–Uhlenbeck model: the exact weighted dissipation identity, mass conservation, semigroup formulation, microscopic velocity coercivity, macroscopic recovery by the torus Poincaré inequality and a direct modified-energy proof of exponential relaxation. The numerical section is also expanded beyond illustration which derives the Fourier–Hermite system, proves a semi-discrete stability identity, compares Fourier and Hermite truncation levels and reports spectral data for the dominant block. The semigroup viewpoint used in the well-posedness part of this paper follows the general theory of one-parameter semigroups [11].

First, flat d-dimensional torus can be set as

$$\mathbb{T}^d = (\mathbb{R}/2\pi\mathbb{Z})^d$$

Throughout our work, integration in x is taken with respect to the normalized Haar measure on $\mathbb{T}^d$, again denoted by dx, so that

$$\int_{\mathbb{T}^d} dx = 1.$$

The unknown is

$$f = f(t,x,v), t \geq 0, x \in \mathbb{T}^d, v \in \mathbb{R}^d,$$

and the equation is

$$\partial_t f + v \cdot \nabla_x f = \gamma \nabla_v \cdot (\nabla_v f + vf), \gamma > 0. \qquad (1)$$

The parameter γ is the velocity relaxation rate. The normalized Maxwellian

$$M(v) = (2\pi)^{-\frac{d}{2}} \exp\left(-\frac{|v|^2}{2}\right) \qquad (2)$$

is stationary, and the total mass determines the final equilibrium.

Equation (1) appears as a force-free kinetic Fokker–Planck or Kramers-type equation. It models particles whose positions are transported by their velocities while the velocity distribution is driven toward a Maxwellian by linear friction and Gaussian fluctuations. The same structure occurs in Langevin dynamics, Brownian motion, collisional relaxation benchmarks and numerical tests for degenerate parabolic solvers. The periodic geometry removes boundary effects and isolates the transfer of velocity relaxation into spatial relaxation.

2. Functional setting

The weighted Hilbert space is defined as

$$H := L^2(\mathbb{T}^d \times \mathbb{R}^d, M(v)^{-1}\, dx\, dv)$$

with inner product

$$\langle f, h \rangle_{M^{-1}} = \int_{\mathbb{T}^d \times \mathbb{R}^d} f(x,v)\ \overline{h(x,v)}\ M(v)^{-1}\, dx\, dv. \qquad (3)$$

The associated norm is denoted by $\|\cdot\|_{M^{-1}}$. It is often clearer to divide out the Maxwellian. We set

$$g = \frac{f}{M}, d\mu(x,v) = dx\, M(v)\, dv. \qquad (4)$$

Then $f \mapsto g$ is an isometry from H onto $L^2(\mu)$, because

$$\| f \|_{M^{-1}}^2 = \int_{\mathbb{T}^d \times \mathbb{R}^d} | g(x,v) |^2 \, d\mu(x,v). \qquad (5)$$

In these variables, equation (1) becomes

$$\partial_t g = \mathcal{L}g, \mathcal{L}g = \gamma(\Delta_v g - v \cdot \nabla_v g) - v \cdot \nabla_x g. \qquad (6)$$

On smooth functions, we write

$$Af := \gamma \nabla_v \cdot (\nabla_v f + vf), Bf := -v \cdot \nabla_x f, L := A + B. \qquad (7)$$

Here we use the core

$$\mathcal{D} = C_{\text{per}}^{\infty}(\mathbb{T}^d; \mathcal{S}(\mathbb{R}^d)), \mathcal{D}_M := M\mathcal{D}, \qquad (8)$$

where $\mathcal{S}(\mathbb{R}^d)$is the Schwartz class in the velocity variable. Thus functions in $\mathcal{D}$ are smooth and periodic in x, with rapid decay in v after multiplication by M.

Proposition 1. Weighted symmetry and skew-symmetry.
By letting $f = Mg$ and $h = Mq$, with $g, q \in \mathcal{D}$, then

$$\langle Af, h \rangle_{M^{-1}} = -\gamma \int_{\mathbb{T}^d \times \mathbb{R}^d} \nabla_v g \cdot \nabla_v \bar{q} \, d\mu, \qquad (9)$$

and

$$\langle Bf, h \rangle_{M^{-1}} = -\int_{\mathbb{T}^d \times \mathbb{R}^d} (v \cdot \nabla_x g) \, \bar{q} \, d\mu = -\langle Bh, \bar{f} \rangle_{M^{-1}}. \qquad (10)$$

Thus, A is symmetric and non-positive in H, while B is skew-symmetric on $\mathcal{D}_M$.

Proof of Proposition 1.
Since $\nabla_v M = -vM$, the identity

$$\nabla_v(Mg) + vMg = M\nabla_v g$$

gives

$$Af = \gamma \nabla_v \cdot (M\nabla_v g).$$

Inserting this expression in (3) and integrating by parts in v proves (9). The boundary term vanishes because Mdecays exponentially and g, q have Schwartz velocity dependence. Formula (10) follows by integration by parts in the periodic variable x, using that $M$is independent of x.

Corollary 2. Dissipation identity.
For every $f = Mg \in \mathcal{D}_M$,

$$\langle Lf, f\rangle_{M^{-1}} = -\gamma \int_{\mathbb{T}^d\times\mathbb{R}^d} |\nabla_v g(x,v)|^2 \; d\mu(x,v). \qquad (11)$$

Equivalently,

$$\langle Lf, f\rangle_{M^{-1}} = -\gamma \int_{\mathbb{T}^d\times\mathbb{R}^d} M(v) \,|\, \nabla_v \left(\frac{f}{M}\right) |^2 \; dx\,dv.$$

Proof of Corollary 2.
Take $h = f$ in Proposition 1. The B-part has zero real contribution and the A-part gives (11).

3. Well-posedness, mass and microscopic coercivity

Theorem 3. Contraction semigroup
The operator L, initially defined on $\mathcal{D}_M$, is closable in H. Its closure, still denoted by L, generates a strongly continuous contraction semigroup $(S_t)_{t\geq 0}$on H. Hence, for every $f_0 \in H$, equation (1) has a unique global mild solution

$$f(t) = S_t f_0 \in C([0,\infty); H),$$

and

$$\| S_t f_0 \|_{M^{-1}} \leq \| f_0 \|_{M^{-1}}, t \geq 0. \qquad (12)$$

Proof of Theorem 3.
Under the isometry $f = Mg$, the operator L is transformed into $\mathcal{L}$in (6). This is the Kolmogorov generator associated with the diffusion

$$dX_t = -V_t\,dt, dV_t = -\gamma V_t\,dt + \sqrt{2\gamma}\,dW_t$$

on $\mathbb{T}^d \times \mathbb{R}^d$. The measure $\mu = dx\,M(v)\,dv$ is invariant. The corresponding Markov semigroup $(P_t)_{t\geq 0}$ is therefore contractive in $L^2(\mu)$ by Jensen's inequality:

$$\| P_t g \|^2_{L^2(\mu)} \leq \int_{\mathbb{T}^d\times\mathbb{R}^d} P_t\,(|\, g \,|^2)\,d\mu = \| g \|^2_{L^2(\mu)}.$$

The smooth periodic-Schwartz class $\mathcal{D}$ is a core for this Ornstein–Uhlenbeck–transport generator. Thus the closure of $\mathcal{L}$ generates $(P_t)_{t\geq 0}$. Returning through the isometry gives $S_t(Mg) = MP_t g$, which proves the theorem.

Remark 1.
Theorem 3 is a standard well-posedness statement for this Kolmogorov operator. The core of this paper is the quantitative decay estimate proved in Section 4.

Proposition 4. Mass and equilibrium.
By letting f be a smooth solution of (1) , we have

$$\frac{d}{dt}\int_{\mathbb{T}^d\times\mathbb{R}^d} f(t,x,v)\,dx\,dv = 0. \qquad (13)$$

If

$$m_0 = \int_{\mathbb{T}^d \times \mathbb{R}^d} f_0\,(x, v)\; dx\, dv,$$

then the corresponding Maxwellian equilibrium is

$$f_\infty(v) = m_0 M(v). \qquad (14)$$

Proof of Proposition 4.
Integrating (1) over $\mathbb{T}^d \times \mathbb{R}^d$, the spatial transport term vanishes by periodicity and the velocity divergence integrates to zero because of the Gaussian decay. Since $\int_{\mathbb{T}^d} dx = 1$ and $\int_{\mathbb{R}^d} M(v)\, dv = 1$, the state in (14) has mass m_0 and is stationary.

The zero-mass space is

$$H_0 = \left\{ f \in H : \int_{\mathbb{T}^d \times \mathbb{R}^d} f\,(x, v)\; dx\, dv = 0 \right\}. \qquad (15)$$

Relaxation to equilibrium is equivalent to decay on H_0, after replacing f by $f - f_\infty$.

Proposition 5. Gaussian Poincaré inequality.
Setting $h \in H^1(\mathbb{R}^d, M\, dv)$ can satisfy

$$\int_{\mathbb{R}^d} h(v) M(v)\, dv = 0.$$

Then

$$\int_{\mathbb{R}^d} |\, h(v)\, |^2\; M(v)\, dv \le \int_{\mathbb{R}^d} |\, \nabla_v h(v)\, |^2\; M(v)\, dv. \qquad (16)$$

Proof of Proposition 5.
This is the standard Poincaré inequality for the centered Gaussian probability measure with covariance identity.

For $f = Mg$, we define the projection onto the local Maxwellian manifold by

$$(\Pi f)(x, v) = M(v) \int_{\mathbb{R}^d} g(x, w) M(w)\, dw. \qquad (17)$$

The projected factor is independent of v. We denote it by

$$\bar{g}(x) = \int_{\mathbb{R}^d} g(x, w) M(w)\, dw.$$

Proposition 6. Microscopic coercivity.
For every $f = Mg \in \mathcal{D}_M$,

$$-\langle Af, f\rangle_{M^{-1}} \geq \gamma \| (\mathrm{Id} - \Pi)f \|_{M^{-1}}^2. \qquad (18)$$

Proof of Proposition 6.
By Eq (9)

$$-\langle Af, f\rangle_{M^{-1}} = \gamma \int_{\mathbb{T}^d\times\mathbb{R}^d} | \nabla_v g |^2 \ d\mu.$$

For each fixed x, the function $g(x,\cdot) - \bar{g}(x)$ has zero Gaussian mean. Applying Proposition 5 and integrating in x gives

$$\int_{\mathbb{T}^d\times\mathbb{R}^d} | g - \bar{g} |^2 \ d\mu \leq \int_{\mathbb{T}^d\times\mathbb{R}^d} | \nabla_v g |^2 \ d\mu.$$

Since $(\mathrm{Id} - \Pi)f = M(g - \bar{g})$, the left-hand side is exactly $\| (\mathrm{Id} - \Pi)f \|_{M^{-1}}^2$.

4. Hypocoercive exponential convergence

We now prove exponential relaxation on the zero-mass subspace. The proof is written for smooth solutions of (6); the estimate then extends by density and Theorem 3. All norms and inner products in this section are taken in $L^2(\mu)$.

Lemma 7. Differential identities.
we let g be a smooth solution of (6). Then

$$\frac{1}{2}\frac{d}{dt} \| g \|^2 = -\gamma \| \nabla_v g \|^2, \qquad (19)$$
$$\frac{1}{2}\frac{d}{dt} \| \nabla_x g \|^2 = -\gamma \| \nabla_v \nabla_x g \|^2, \qquad (20)$$
$$\frac{1}{2}\frac{d}{dt} \| \nabla_v g \|^2 = -\gamma \| \nabla_v^2 g \|^2 - \gamma \| \nabla_v g \|^2 - \langle \nabla_x g, \nabla_v g\rangle, \qquad (21)$$

and

$$\frac{d}{dt}\langle \nabla_x g, \nabla_v g\rangle = -\| \nabla_x g \|^2 - \gamma\langle \nabla_x g, \nabla_v g\rangle - 2\gamma\langle \nabla_v \nabla_x g, \nabla_v^2 g\rangle. \qquad (22)$$

Proof of Lemma 7.
The operator $v \cdot \nabla_x$ is skew-symmetric in $L^2(\mu)$, while $\Delta_v - v \cdot \nabla_v$ is symmetric and non-positive with Dirichlet form $\| \nabla_v \cdot \|^2$. This gives (19). Since ∇_x commutes with both parts of $\mathcal{L}$, the same argument applied to $\nabla_x g$ proves (20).

For the velocity derivative, we use

$$[\nabla_v, v \cdot \nabla_x] = \nabla_x, [\nabla_v, \Delta_v - v \cdot \nabla_v] = -\nabla_v.$$

Thus

$$\partial_t \nabla_v g + v \cdot \nabla_x \nabla_v g + \nabla_x g = \gamma(\Delta_v - v \cdot \nabla_v)\nabla_v g - \gamma \nabla_v g.$$

Taking the inner product with $\nabla_v g$ gives (21). Finally, differentiating $\langle \nabla_x g, \nabla_v g \rangle$ in time and inserting the differentiated equations yields (22); the transport contributions cancel by skew-symmetry.

Lemma 8. Recovery of the macroscopic part.
First, let $g \in H^1(\mathbb{T}^d \times \mathbb{R}^d, \mu)$ have zero mean,

$$\int_{\mathbb{T}^d \times \mathbb{R}^d} g \, d\mu = 0.$$

Then

$$\| g \|^2 \leq \| \nabla_v g \|^2 + C_{\mathbb{T}} \| \nabla_x g \|^2, \qquad (23)$$

where $C_{\mathbb{T}}$ is the Poincaré constant of the flat torus with normalized measure.

Proof of Lemma 8.
we set

$$\rho(x) = \int_{\mathbb{R}^d} g(x, v) M(v) \, dv.$$

The zero-mean assumption implies

$$\int_{\mathbb{T}^d} \rho(x) \, dx = 0.$$

The torus Poincaré inequality and Jensen's inequality give

$$\| \rho \|_{L^2(\mathbb{T}^d)}^2 \leq C_{\mathbb{T}} \| \nabla_x \rho \|_{L^2(\mathbb{T}^d)}^2 \leq C_{\mathbb{T}} \| \nabla_x g \|^2.$$

The decomposition $g = (g - \rho) + \rho$ is orthogonal in $L^2(\mu)$. Applying the Gaussian Poincaré inequality in v to $g(x, \cdot) - \rho(x)$ gives

$$\| g - \rho \|^2 \leq \| \nabla_v g \|^2.$$

Adding the two bounds proves Eq (23).

By choosing

$$c_0 = \frac{1}{16} \min\{\gamma, \gamma^{-1}, 1\}, b_0 = \frac{\gamma c_0}{2}, a_0 = 1. \qquad (24)$$

For a smooth function g, we define

$$\mathcal{E}(g) = \| g \|^2 + a_0 \| \nabla_x g \|^2 + b_0 \| \nabla_v g \|^2 + 2c_0 \langle \nabla_x g, \nabla_v g \rangle. \qquad (25)$$

Theorem 9. Hypocoercive decay.
There exist constants $C \geq 1$ and $\lambda > 0$, depending only on d, γ, and the torus, such that every smooth zero-mean solution of (6) satisfies

$$\mathcal{E}(g(t)) \leq Ce^{-\lambda}\ \mathcal{E}(g(0)), t \geq 0. \qquad (26)$$

As a result, for $f = Mg$ and $f_0 \in H_0$ with finite first-order hypocoercive energy,

$$\| f(t) \|_{M^{-1}}^2 \leq Ce^{-\lambda}\ \| f_0 \|_{H^1_{\text{hyp}}}^2. \qquad (27)$$

Proof of Theorem 9.
The choice (24) makes $\mathcal{E}$ equivalent to the first-order norm

$$\| g \|^2 + \| \nabla_x g \|^2 + \| \nabla_v g \|^2.$$

Indeed,

$$2c_0 \mid \langle \nabla_x g, \nabla_v g \rangle \mid \leq \frac{1}{2} \| \nabla_x g \|^2 + 2c_0^2 \| \nabla_v g \|^2,$$

and $2c_0^2 \leq b_0/2$.

We differentiate (25) and use Lemma 7. With

$$X = \| \nabla_x g \|, V = \| \nabla_v g \|, X_v = \| \nabla_v \nabla_x g \|, V_v = \| \nabla_v^2 g \|,$$

one obtains

$$\begin{aligned}\frac{d}{dt}\mathcal{E}(g) \leq \quad & -2\gamma(1 + b_0)V^2 - 2\gamma X_v^2 - 2b_0\gamma V_v^2 - 2c_0 X^2 \\ & +2(b_0 + c_0\gamma) \mid \langle \nabla_x g, \nabla_v g \rangle \mid +4c_0\gamma \mid \langle \nabla_v \nabla_x g, \nabla_v^2 g \rangle \mid.\end{aligned}$$

The last two terms are absorbed by Young's inequality. First,

$$4c_0\gamma \mid \langle \nabla_v \nabla_x g, \nabla_v^2 g \rangle \mid \leq \gamma X_v^2 + 4c_0^2\gamma V_v^2 \leq \gamma X_v^2 + b_0\gamma V_v^2.$$

Second, because $b_0 = \gamma c_0/2$,

$$2(b_0 + c_0\gamma) \mid \langle \nabla_x g, \nabla_v g \rangle \mid \leq c_0 X^2 + \frac{9\gamma^2 c_0}{4} V^2.$$

The restriction $c_0 \leq (16\gamma)^{-1}$gives

$$\frac{9\gamma^2 c_0}{4} \leq \gamma.$$

Hence

$$\frac{d}{dt}\mathcal{E}(g) \leq -c_0 \parallel \nabla_x g \parallel^2 - \gamma \parallel \nabla_v g \parallel^2. \qquad (28)$$

For zero-mean g, Lemma 8 controls $\parallel g \parallel^2$by the two gradient terms. Combining this control with the norm equivalence of $\mathcal{E}$ yields a constant $\lambda > 0$ such that

$$\frac{d}{dt}\mathcal{E}(g(t)) \leq -\lambda\mathcal{E}(g(t)).$$

Grönwall's lemma proves (26). Formula (27) follows from the isometry (5).

5. Spatially homogeneous entropy law

When f is independent of x, equation (1) reduces to the Ornstein–Uhlenbeck Fokker–Planck equation

$$\partial_t f = \gamma\nabla_v \cdot (\nabla_v f + vf), v \in \mathbb{R}^d. \qquad (29)$$

By assuming $f(t,\cdot) > 0$ and

$$\int_{\mathbb{R}^d} f(t,v)\, dv = 1.$$

We define the relative entropy and Fisher information by

$$\mathcal{H}(f \mid M) = \int_{\mathbb{R}^d} f(v) \log \left(\frac{f(v)}{M(v)}\right) dv, \qquad (30)$$

and

$$\mathcal{I}(f \mid M) = \int_{\mathbb{R}^d} f(v) \mid \nabla_v \log \left(\frac{f(v)}{M(v)}\right) |^2 \; dv. \qquad (31)$$

Proposition 10. Entropy dissipation.
Every smooth positive probability solution of (29) satisfies

$$\frac{d}{dt}\mathcal{H}(f(t) \mid M) = -\gamma\mathcal{I}(f(t) \mid M). \qquad (32)$$

Proof of Proposition 10.
Differentiating (30) in time and using conservation of mass gives

$$\frac{d}{dt}\mathcal{H}(f \mid M) = \int_{\mathbb{R}^d} \partial_t f \log \left(\frac{f}{M}\right) dv.$$

We insert (29). Since

$$\nabla_v f + vf = f\nabla_v \log \left(\frac{f}{M}\right),$$

integration by parts gives (32).

Theorem 11. Homogeneous entropy decay.
Every smooth positive probability solution of (29) satisfies

$$\mathcal{H}(f \mid M) \leq \frac{1}{2}\mathcal{I}(f \mid M) \qquad (33)$$

and therefore

$$\mathcal{H}(f(t) \mid M) \leq e^{-2\gamma t}\mathcal{H}(f(0) \mid M), t \geq 0. \qquad (34)$$

Proof of Theorem 11.
Inequality (33) is the Gaussian logarithmic Sobolev inequality. Combining it with Proposition 10 yields

$$\frac{d}{dt}\mathcal{H}(f(t) \mid M) \leq -2\gamma\mathcal{H}(f(t) \mid M).$$

The conclusion follows from Grönwall's lemma.

6. Numerical validation

In this section, we examine the one-dimensional case $d = 1$. The purpose is to verify that the finite-dimensional Fourier–Hermite model reproduces the decay mechanism proved above and to quantify the effect of the truncation parameters. All numerical values reported here were computed with Python 3.11 using NumPy and SciPy; each finite block was evolved by matrix exponentiation.

For $g = f/M$, the equation is

$$\partial_t g + v\,\partial_x g = \gamma(\partial_{vv} g - v\,\partial_v g), (x, v) \in \mathbb{T} \times \mathbb{R}. \qquad (35)$$

So let $\{\varphi_n\}_{n\geq 0}$ be the orthonormal Hermite basis of $L^2(\mathbb{R}, M(v)\,dv)$, normalized so that

$$(\partial_{vv} - v\,\partial_v)\varphi_n = -n\varphi_n, v\varphi_n = \sqrt{n+1}\,\varphi_{n+1} + \sqrt{n}\,\varphi_{n-1}, \qquad (36)$$

with $\varphi_{-1} = 0$. The truncated expansion is

$$g_{K,N}(t, x, v) = \sum_{|k|\leq K} \sum_{n=0}^{N} c_{k,n}(t)e^{ikx}\varphi_n(v). \qquad (37)$$

Substitution in (35) gives, for $\mid k \mid \leq K$ and $0 \leq n \leq N$,

$$\dot{c}_{k,n} = -\gamma n\, c_{k,n} - ik\sqrt{n+1}\, c_{k,n+1} - ik\sqrt{n}\, c_{k,n-1}, \qquad (38)$$

with boundary conventions $c_{k,-1} = c_{k,N+1} = 0$.

The numerical test uses

$$g_0(x,v) = 1 + 0.25\cos\ x + 0.20\ v\sin\ x. \tag{39}$$

The non-equilibrium part occupies only the Fourier modes $k = \pm 1$ and Hermite levels $n = 0{,}1$, while the subsequent evolution transfers mass to higher Hermite levels through the tri-diagonal coupling in (38). The parameters are listed in Table 1.

Table 1. Parameters used in the Fourier–Hermite computation.

Quantity	Value
Relaxation parameter	$\gamma = 1$
Spatial domain	$\mathbb{T} = \mathbb{R}/2\pi\mathbb{Z}$, normalized measure
Reference Fourier truncation	$K_{\text{ref}} = 6$
Reference Hermite truncation	$N_{\text{ref}} = 60$
Displayed Hermite truncation	$N = 15$
Time interval	$0 \le t \le 8$
Initial datum	$g_0(x,v) = 1 + 0.25\cos\ x + 0.20\ v\sin\ x$

For fixed k, write $c_k = (c_{k,0}, \dots, c_{k,N})^\top$. Then (38) has the matrix form

$$\dot{c}_k = A_{k,N} c_k,$$

where

$$(A_{k,N})_{nn} = -\gamma n, (A_{k,N})_{n,n+1} = -ik\sqrt{n+1}, (A_{k,N})_{n,n-1} = -ik\sqrt{n}. \tag{40}$$

Proposition 12. Semi-discrete stability.
For every $k \in \mathbb{Z}$ and $N \ge 0$, the truncated Fourier–Hermite block satisfies

$$\frac{1}{2}\frac{d}{dt}\sum_{n=0}^{N} |\, c_{k,n}(t)\, |^2 = -\gamma \sum_{n=0}^{N} n\ |\, c_{k,n}(t)\, |^2 \le 0. \tag{41}$$

Proof of Proposition 12.
The diagonal part of $A_{k,N}$ is real and non-positive. The off-diagonal part is skew-Hermitian because its upper and lower entries are conjugate with opposite sign. Taking the real part of $\langle A_{k,N} c_k, c_k \rangle_{\mathbb{C}^{N+1}}$ gives exactly (41).

The Fourier truncation is transparent in this test. Since (35) is diagonal in k and (39) contains no spatial modes beyond $0, \pm 1$, every truncation $K \ge 1$ gives the same result up to round-off error. **Table 2** reports this fact using $K_{\text{ref}} = 6$ and $N = 15$.

Table 2. Fourier truncation error relative to $K_{\text{ref}} = 6$ with $N = 15$.

K	Fourier modes retained from the initial datum	$\max_{0\le t\le 8} \| g_{K,15}(t) - g_{6,15}(t) \|_{L^2(\mu)}$
0	only $k = 0$	2.264×10^{-1}
1	$k = 0, \pm 1$	$<10^{-14}$
2	$k = 0, \pm 1$	$<10^{-14}$
4	$k = 0, \pm 1$	$<10^{-14}$
6	reference	0

The Hermite truncation is the relevant numerical parameter. For $N < N_{\text{ref}}$, we define

$$E_N(t) = \left(\sum_{|k|\le 1} \sum_{n=0}^{60} | c_{k,n}^{(N)}(t) - c_{k,n}^{(60)}(t) |^2 \right)^{1/2}, \qquad (42)$$

where $c_{k,n}^{(N)} = 0$ for $n > N$. **Figure 1** displays a rapid convergence as N increases on a logarithmic scale.

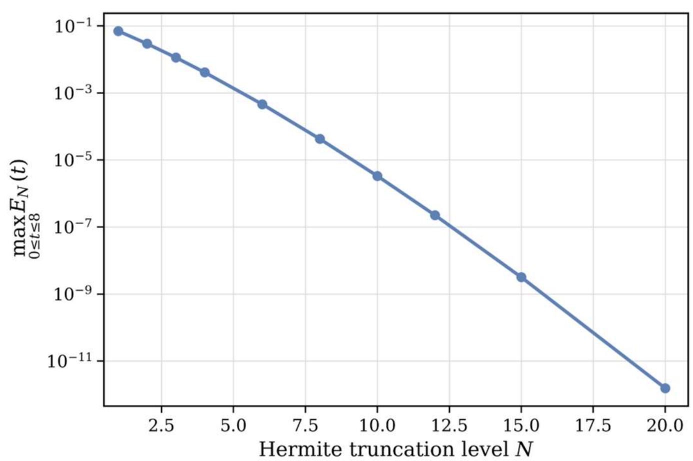

Figure 1. Hermite truncation convergence

The next diagnostic is the weighted distance from equilibrium,

$$\| f(t) - M \|_{M^{-1}} = \| g(t) - 1 \|_{L^2(\mu)}.$$

For $K = 6$ and $N = 15$, a least-squares fit of $\log \| g(t) - 1 \|_{L^2(\mu)}$ over $1 \le t \le 8$ gives the slope -1.091. **Figure 2** shows the computed curve and the fitted exponential line.

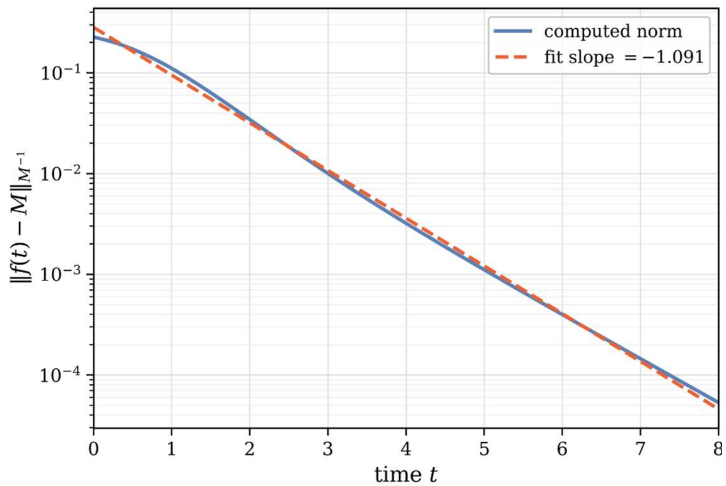

Figure 2. Weighted relaxation to equilibrium

The long-time decay is governed by the rightmost eigenvalues of the nonzero Fourier blocks. **Figure 3** shows the spectral abscissa

$$\alpha_{1,N} := \max \{\text{Re } \lambda : \lambda \in \sigma(A_{1,N})\}$$

for the first nonzero block. The values approach -1 and indicates the spectral localization for $N = 15$.

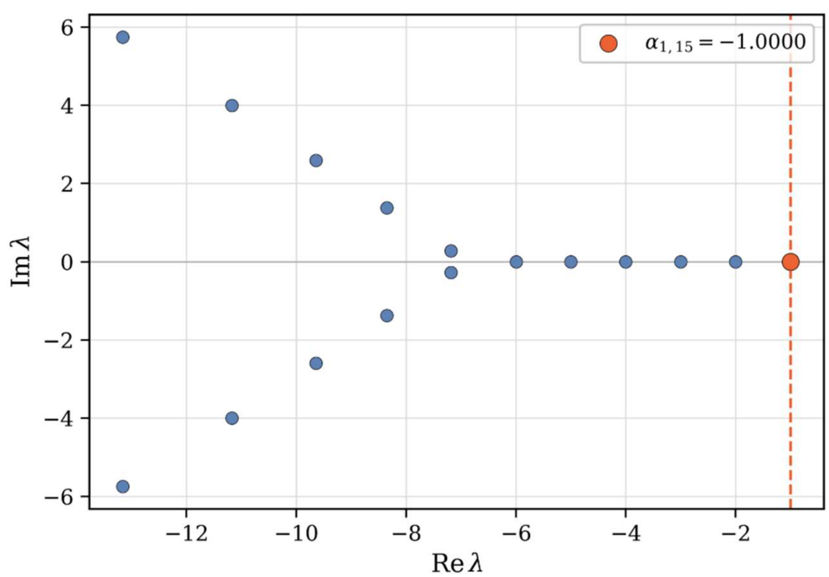

Figure 3. Spectrum of the truncated first Fourier block $A_{1,15}$

Lastly, the macroscopic density

$$\rho(t,x) = \int_{\mathbb{R}} f(t,x,v)\, dv$$

isolates the zeroth Hermite coefficient. **Figure 4** plots $\rho(t,x) - 1$ at four times. The amplitude decreases from 2.500×10^{-1}at $t = 0$ to 2.623×10^{-3}at $t = 4$, with no visible high-frequency contamination.

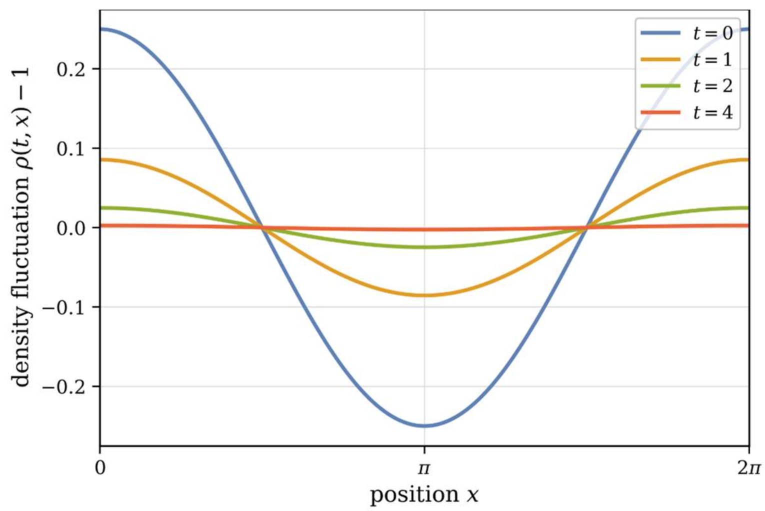

Figure 4. Macroscopic density snapshots

7. Conclusion

This paper gives a complete treatment of the periodic transport–Ornstein–Uhlenbeck equation (1) in the weighted L^2 setting. The Maxwellian change of variables exposes the structure of the generator which the velocity part is symmetric and dissipative while the spatial transport part is skew-symmetric. The resulting contraction semigroup preserves mass and the equilibrium is the Maxwellian with the same total mass as the initial datum. The proof uses two elementary coercive ingredients: the Gaussian Poincaré inequality controls the velocity fluctuation around the local Maxwellian and the torus Poincaré inequality controls the remaining spatial average. A modified first-order energy with a single mixed derivative term links these two controls and yields global decay. The homogeneous entropy calculation is consistent with the same relaxation scale through the Gaussian logarithmic Sobolev inequality. The Fourier–Hermite computation provides an independent modal check of the analysis. The discrete system is stable, the Fourier truncation is exact once $K \geq 1$ for the chosen datum, the Hermite truncation error decays rapidly with N and the spectrum of the first nonzero Fourier block identifies the observed long-time rate. These results make the model a clean benchmark for hypocoercive analysis and for spectral discretizations of kinetic Fokker–Planck equations.

Acknowledgements

We are grateful to the **Visous Time Theory team (VTT)** for their valuable feedback on this version. Their comments helped improve the clarity, structure, and presentation of the work.

References

[1] T. D. Frank, "Linear and Nonlinear Fokker-Planck Equations," *Synergetics*, pp. 149–182, 2020, doi: 10.1007/978-1-0716-0421-2_311.

[2] A. Kolmogoroff, "Zufallige Bewegungen (Zur Theorie der Brownschen Bewegung)," *The Annals of Mathematics*, vol. 35, no. 1, p. 116, Jan. 1934, doi: 10.2307/1968123.

[3] H. A. Kramers, "Brownian motion in a field of force and the diffusion model of chemical reactions," *Physica*, vol. 7, no. 4, pp. 284–304, Apr. 1940, doi: 10.1016/S0031-8914(40)90098-2.

[4] L. Hörmander, "Hypoelliptic second order differential equations," *Acta Mathematica 1967 119:1*, vol. 119, no. 1, pp. 147–171, Dec. 1967, doi: 10.1007/BF02392081.

[5] L. Gross, “Logarithmic Sobolev Inequalities,” *American Journal of Mathematics*, vol. 97, no. 4, p. 1061, Winter 1975, doi: 10.2307/2373688.

[6] H. Risken, “The Fokker-Planck Equation,” vol. 18, 1996, doi: 10.1007/978-3-642-61544-3.

[7] F. Hérau and F. Nier, “Isotropic Hypoellipticity and Trend to Equilibrium for the Fokker-Planck Equation with a High-Degree Potential,” *Arch. Ration. Mech. Anal.*, vol. 171, no. 2, pp. 151–218, Oct. 2004, doi: 10.1007/S00205-003-0276-3/METRICS.

[8] C. Mouhot and L. Neumann, “Quantitative perturbative study of convergence to equilibrium for collisional kinetic models in the torus,” *Nonlinearity*, vol. 19, no. 4, p. 969, Mar. 2006, doi: 10.1088/0951-7715/19/4/011.

[9] H. Cédric Villani, “Hypocoercivity,” *Mem. Am. Math. Soc.*, vol. 202, no. 950, pp. 0–0, Sep. 2006, doi: 10.1090/s0065-9266-09-00567-5.

[10] J. Dolbeault, C. Mouhot, and C. Schmeiser, “Hypocoercivity for linear kinetic equations conserving mass,” *Trans. Am. Math. Soc.*, vol. 367, no. 6, pp. 3807–3828, Feb. 2015, doi: 10.1090/S0002-9947-2015-06012-7.

[11] “One-Parameter Semigroups for Linear Evolution Equations,” *One-Parameter Semigroups for Linear Evolution Equations*, 2000, doi: 10.1007/B97696.

Dear reader, thank you for taking the time to read this paper. We would be happy to hear your thoughts, comments or suggestions. Please feel free to contact by email.

With best regards,

©Payam Danesh

©Raoul Bianchetti